BOLETIN LATINOAMERICANO Y DEL CARIBE DE PLANTAS MEDICINALES Y AROMÁTICAS
© / ISSN 0717 7917 / www.blacpma.ms-editions.cl

Articulo Original / Original Article

Development, characterization and anti-*Mycobacterium tuberculosis* activity of solid lipid nanoparticles for oral *Piper corcovadensis* roots extract delivery

[Desarrollo, caracterización y actividad anti-*Mycobacterium tuberculosis* de nanopartículas lipídicas sólidas para la administración oral de extracto de raíces de *Piper corcovadensis*]

Carla María Mariano Fernandez[1], Sirlene Adriana Kleinubing[1], Thaysa Ksiaskiewcz Karam[1], Fabiana Brusco Lorenzetti[1], Carolina Trevisolli Palomo[2], Byanca Pereira Moreira de Oliveira[3], Odinei Hess Gonçalves[3], Zilda Cristiani Gazim[4], Mariza Barion Romagnolo[5], Katiany Rizzieri Caleffi-Ferracioli[2], Regiane Bertin de Lima Scodro[6], Marli Miriam de Souza Lima[1], Tânia Ueda Nakamura[1], Celso Vataru Nakamura[1] & Benedito Prado Dias Filho[1]

[1]Postgraduate Program in Pharmaceutical Sciences, State University of Maringá (UEM), Maringá, Brazil
[2]Postgraduate Program in Biosciences and Pathophysiology, UEM, Maringá, Brazil
[3]Postgraduate Program of Food Technology, Federal University of Technology - Paraná, Campo Mourão, Paraná, Brazil
[4]Postgraduate Program in Biotechnology Applied to Agriculture, Paranaense University, Umuarama, Paraná, Brazil
[5]Departament of Biology, UEM, Maringá, Brazil
[6]Postgraduate Program in Health Sciences, UEM, Maringá, Brazil

Reviewed by:
Juan Bueno
Fundación BIOLABB
Colombia

Ignacio Agudelo
Universidad de Buenos Aires
Argentina

Correspondence:
Benedito Prado **DIAS FILHO**:
bpdfilho@uem.br

Section Biological activity

Received: 15 June 2022
Accepted: 8 October 2022
Accepted corrected: 28 December 2022
Published: 30 November 2023

Citation:
Fernandez CMM, Kleinubing SA, Karam TK, Lorenzetti FB, Palomo CT, Oliveira BPM, Gonçalves OH, Gazim ZC, Romagnolo MB, Ferracioli KRC, Scodro RBL, Lima MMS, Nakamura TU, Nakamura CV, Filho BPD Development, characterization and anti-Mycobacterium tuberculosis activity of solid lipid nanoparticles for oral Piper corcovadensis roots extract delivery
Bol Latinoam Caribe Plant Med Aromat 22 (6): 821 - 836 (2023).
https://doi.org/10.37360/blacpma.23.22.6.55

Abstract: The present study thus aimed at the development and physicochemical characterization of solid lipid nanoparticles loaded with crude extract of *Piper corcovadensis* roots (SLN-CEPc) and chitosan-coated solid lipid nanoparticles loaded with crude extract of *P. corcovadensis* roots (C-SLN-CEPc), as well as the determination of its antimycobacterial activity against *Mycobacterium tuberculosis* H37Rv, its cytotoxicity against the Vero cell line and evaluation in the hemolysis assay. Both formulations containing the encapsulated extract showed high encapsulation efficiency, formed by a monodispersed system with small and spherical particles, and there was no aggregation of particles. In the biological assays, SLN-CEPc and C-SLN-CEPc showed promising anti-*M. tuberculosis* activity with a minimum inhibitory concentration (MIC) of 12.5 µg/mL, whereas the cytotoxic concentrations obtained at 50% (CC_{50}) in Vero cells were 60.0 and 70.0 µg/mL, respectively. Therefore, nanoencapsulation showed satisfactory results, justifying its usage in the development of new products.

Keywords: Solid lipid nanoparticles; *Piper corcovadensis*; Tuberculosis; Chitosan; Cytotoxicity

Resumen: El presente estudio apuntó al desarrollo y caracterización fisicoquímica de nanopartículas lípidas en estado sólido, cargadas con extracto crudo de raíz de *Piper corcovadensis* (SLN-CEPc) y nanopartículas lípidas en estado sólido cubiertas con quitosano cargadas con extracto crudo de raíz de *P. corcovadensis* (C-SLN-CEPc), así como la determinación de su actividad antimicobacterial contra *Mycobacterium tuberculosis* H37Rv, su citotoxicidad contra la línea celular Vero y su evaluación en ensayo de hemólisis. Ambas formulaciones que contenían el extracto encapsulado mostraron alta eficiencia de encapsulación, formado por un sistema monodispersado con pequeñas partículas esféricas, y no hubo agregación de partículas. En los ensayos biológicos, SLN-CEPc y C-SLN-CEPc mostraron una prometedora actividad anti-*M. tuberculosis* con una mínima concentración inhibitoria (MIC) de 12,5 µg/mL, mientras que las concentraciones citotóxicas obtenidas al 50% (CC_{50}) en células Vero estuvo en 60,0 y 70,0 µg/mL, respectivamente. Por lo tanto, la nanoencapsulación mostró resultados satisfactorios, justificando su uso en el desarrollo de nuevos productos.

Palabras clave: Nanopartículas lípidas en estado sólido; *Piper corcovadensis*; Tuberculosis; Quitosan; Citotoxicidad.

INTRODUCTION

Tuberculosis (TB) is an infectious disease caused by the bacillus *Mycobacterium tuberculosis* which usually affects the lungs (pulmonary tuberculosis), transmitted by the inhalation of droplets containing expelled bacilli from the coughing, speaking, or sneezing of a patient with active tuberculosis (WHO, 2019). According to World Health Organization (WHO, 2019), in 2018, it was estimated that 10.0 million people falling ill with tuberculosis worldwide, with approximately 1.5 million deaths, remains the top infectious killer worldwide, and reports that about 3 million people with TB did not have access quality health care.

The World Health Organization, from an epidemiological point of view, estimated that about 1.7 billion people are infected with *M. tuberculosis*, and 5-10% of these people will develop the disease during their lifetime (WHO, 2019). Another concern is the increase in drug-resistant TB cases (WHO, 2019), so urgent action is needed to improve and increase the number of drugs that have effective action against *M. tuberculosis*. In this way, researchers have been developing research projects with plants looking for new classes of antimycobacterial agents (Scodro *et al*., 2015; Pereira *et al*., 2018; Fernandez *et al*., 2019).

The species *Piper corcovadensis* (Piperaceae), popularly known as "João brandinho" and "Falso-jaborandi", it is a Brazilian native shrub commonly used for the treatment of flu, cough, and rheumatism (Parmar *et al*., 1997; Facundo *et al*., 2004). In the studies by Fernandez *et al*. (2019), the *P. corcovadensis* root extract showed potential anti-tuberculosis activity against *Mycobacterium tuberculosis* $H_{37}Rv$ and for resistant clinical isolates, as well as a synergistic effect with isoniazid and rifampicin. However, the extract of *P. corcovadensis* has low water solubility, a limiting factor for the oral bioavailability, being one of the main challenges in the pharmaceutical field, the employment of molecules with therapeutic potential as drugs. Thus, nanotechnology is an alternative that has enabled effective administration and the modified release of the active molecule according to the needs of the patients and the characteristics of the drug (Jato, 2009; Marcato, 2009; Trousil *et al*., 2017).

Solid lipid nanoparticles are nanocarriers formed by solid lipids at room and body temperature and are stabilized by one or more surfactants. In these systems, the drug is encapsulated in a lipid matrix covered by a phospholipid monolayer (Marcato, 2009; Geszke-Moritz & Moritz, 2016). Solid lipid nanoparticles present several benefits in the oral release of drugs, such as: (1) encapsulation of lipophilic and hydrophilic drugs; (2) increase in permeability and bioavailability in the epithelium; (3) protection of the active molecule in the storage and during oral administration of photosensitive, moisture-sensitive and chemically labile molecules; (4) viability of industrial production due to the low cost and simplicity and (5) low toxicity (Marcato, 2009; Das & Chaudhury, 2011; Lin *et al*., 2017). Furthermore, they might have potential applications in the pharmaceutical area, such as against diseases of the central nervous system, cardiovascular and inflammatory diseases, cancer, and viral and bacterial infections (Marcato, 2009; Lin *et al*., 2017).

Surface modifications of solid lipid nanoparticles may improve the biocompatibility and the interaction of these systems with the target site (Mishra *et al*., 2018). Chitosan is a natural cationic, biodegradable, biocompatible, and low toxicity polysaccharide, which can be used to coat solid lipid nanoparticles by adsorption through electrostatic interactions with the negative surface of solid lipid nanoparticles (Baek & Cho, 2017). Besides that, it has mucoadhesive properties, promoting greater interaction, adhesion, and retention of the pharmaceutical form in the intestinal epithelium (Lima *et al*., 2018).

Whereas the application of the crude extract of *P. corcovadensis* would have several limitations due to its hydrophobic characteristic, which would affect bioavailability, the present study thus aimed to develop, characterize and evaluate the anti-tuberculosis activity in *Mycobacterium tuberculosis* $H_{37}Rv$ of solid lipid nanoparticles containing crude extract of *P. corcovadensis* roots. The nanoparticles were obtained with and without chitosan coating by the method of melt-emulsification and were evaluated for cytotoxicity using Vero cells and hemolysis assay.

MATERIALS AND METHODS

Materials

Precirol® ATO and phospholipon 90G were kindly supplied by Gatefossé (France) and Lipoid (Germany), respectively. The PEG 40 hydrogenated castor oil with 40 moles of ethylene oxide was purchased from the company Oxiteno. Sorbitan monooleate (Span® 80) and isoniazid were obtained from Sigma-Aldrich, whereas Piperlonguminine >

98% was purchased from Cayman Chemical. Acetonitrile, formic acid, and HPLC grade chloroform were purchased from Panreac. The ultra-pure water used was obtained by the Milli-Q purification system (Millipore®).

High-performance liquid chromatography (HPLC) with photodiode array (PDA)

The analysis was carried out by high-performance liquid chromatography (Waters 2695) with photodiode array (Waters 2998) (HPLC-PDA) by using the software Empower® to obtain the data. The separation was performed on a Hyperclone C18 column (5 µ ODS, 250 x 4.6 mm) (Phenomenex®, USA) with a KJO-4282 pre-column (particle ≥ 3 µm, < 5,000 psi / 345 bar) (Phenomenex®, USA). The injection volume was 20 µL and the UV-vis detection system was 332 nm. As mobile phase, water was acidified with formic acid at 0.1% (phase A) and acetonitrile acidified with formic acid at 0.1% (phase B) with a flow rate of 1.0 mL/min. The phase A:B was constituted as follows: 95:5 for 10 minutes, 40:60 from 10 to 18 minutes, and 5:95 up to 24 minutes, with an analysis time of 24 minutes. Prior to the analysis, the samples were solubilized in chloroform and filtered by using an HV membrane (Durapore) in a PVDF of 0.45 µm (Millipore®, USA).

Analytical curve of Piperlonguminine

The calibration curve was determined within the range from 5.00 to 0.06 µg/mL. Solutions were prepared in triplicate at different concentrations (5.00; 2.50; 1.25; 0.50; 0.25; 0.12 and 0.06 µg/mL) from a piperlonguminine stock solution (1 mg/mL). The peak areas related to piperlonguminine were plotted along with the respective concentrations (data not shown). The linearity estimated by linear regression showed a coefficient of determination (r^2) of 0.9999, which is in accordance with the limit (> 0.99) specified by Resolution RE nº 166, from July, 24th 2017 (Brasil, 2017). Thus, it can be said that there is a correlation between the peak area and the concentration of analyte within the evaluated concentration range.

Plant material and collection of the crude extract

The roots of *P. corcovadensis* were collected at the Caiuá Ecological Station (52º 49' to 52º53'W and 22º 34'to 22º 37' S), Diamante do Norte, Paraná, Brazil. The exsiccate was identified by Dr. Mariza Barion Romagnolo and placed at the Herbarium of Nupélia under the number 16706. The roots were then dried in a circulating air oven (Quimis®) at 40ºC and then sprayed in a knife mill (Usi Ram). The root powder (350 g) was subjected to extraction in a Soxhlet apparatus by using dichloromethane as extracting solvent for 2 hours. After that, the crude extract of *P. corcovadensis* roots (CEPc) was concentrated under reduced pressure in a rotary evaporator at 40ºC (IKA® RV 10 Basic) and then stored at 4ºC (Fernandez *et al*., 2019).

Production of the solid lipid nanoparticles (SLN)

The solid lipid nanoparticles were prepared by the method of melt-emulsification followed by cooling. The oil phase, which was composed of the lipid (Precirol® ATO 5, 1.5%), lipophilic surfactants (Phospholipon 90G, 1.0% e Span® 80, 1.0%), and CEPc (0.5%), was heated to 90ºC. The aqueous phase, composed by water and the hydrophilic surfactant (PEG 40H, 7.0%), was heated up to the same temperature as the oil phase. The oil phase was poured over the aqueous phase with constant agitation of 15,000 rpm in the Ultra-Turrax® (IKA®T25, USA) for 10 minutes. The formulation was then cooled to room temperature in an ice bath to solidify the lipid, obtaining the solid lipid nanoparticles loaded with crude extract of *Piper corcovadensis* roots (SLN-CEPc). The solid lipid nanoparticles without CEPc (SLN) were prepared by following this same methodology.

SLN-coating with chitosan

The SLN-CEPc were coated with chitosan by physical adsorption following, with some alterations, the methodology described by Baek and Cho (2017). For that, equal volumes of negatively charged SLN or SLN-CEPc and chitosan solution (0.2% in 0.2% acetic acid) were mixed and stirred at 200 rpm for 30 min. The resulting chitosan-coated solid lipid nanoparticles loaded with crude extract of *P. corcovadensis* roots (C-SLN-CEPc) were stored at 4°C. The chitosan-coated solid lipid nanoparticles without CEPc (C-SLN) were also prepared following this same methodology.

Characterization of the SLN

The formulations were visually analyzed in terms of color, appearance, and phase separation. The determinations of average diameter and polydispersity index of the nanoparticles were performed by the scattered light method, whereas the Zeta potential was obtained by the electrostatic mobility method, both at the temperature of 25±0.1ºC using the equipment Litesizer 500 Particle Analyzer

(Anton Paar, USA). To perform the measurements, the samples were diluted in ultra-pure water at the by volume-proportion of 1:10. Both SLN-CEPc and C-SLN-CEPc were stored and kept at temperatures of 5ºC, 30ºC, and 40ºC for 90 days. At pre-determined intervals (15, 30, 60, and 90 days) the samples were analyzed in terms of macroscopic aspects, such as transparency, viscosity and uniformity, average diameter, polydispersity index (PI), and Zeta potential. The stability study was carried based on the guide for the realization of stability Resolution RE No. 1, from July, 29th 2005 (Brasil, 2005). To assess the stability of SLN-CEPc and C-SLN-CEPc at different pH ranges, the nanoparticle suspensions were dissolved in water with previously adjusted pH (3.0; 5.0; 6.0; 7.0 and 9.0) so that the average diameter and the Zeta potential could be analyzed. The pH of the samples was determined using a pH meter (Digimed DM 22) at 25±1ºC.

Moreover, the encapsulation efficiency (EE) was determined by the indirect method, concerning the quantification of free piperlonguminine present in SLN-CEPc and C-SLN-CEPc as follows: the nanoparticle suspension was submitted to ultrafiltration/centrifugation. A 250 µL aliquot of the nanoparticle suspension was then subjected to centrifugation (Eppendorf 5810 R) in a 30 kDa ultra-filter of regenerated cellulose (Amicon 0.5 mL - Millipore®) at 3,500 rpm for 45 minutes (3 washes with ultra-purified water every 15 minutes). The ultra-filtrate was analyzed by HPLC-PDA and the concentration of free piperlonguminine was then determined. The encapsulation efficiency (EE%) was calculated by using Equation 1, where $m_{CEPc\ actual}$ is the mass of CEPc detected by HPLC-PDA in the sample and $m_{CEPc\ added}$ is the theoretical mass of CEPc added according to the formulation.

$$EE\ (\%) = 100.\frac{m_{CEPc\ actual}}{m_{CEPc\ added}} \qquad (1)$$

The amount of CEPc incorporated in the prepared SLN-CEPc and C-SLN-CEPc was determined by the ratio between the mass of CEPc present in the nanoparticle suspension and the mass of nanoparticle suspension weighed for the determination, multiplied by 100. The result was presented as a percentage of incorporation.

The morphology and homogeneity of both SLN-CEPc and C- SLN-CEPc were observed under the transmission electron microscopy (TEM) (JEM - 1400, JEOL). A volume of 10 µL of formulation was placed on a copper grid, covered with carbon film and then kept at rest for 5 min. After that, the excess water was removed with filter paper, and 10 µL of phosphotungstic acid at 2.0% (m/v) was applied for the contrast, and then kept at rest for 10 min. The grid was subsequently kept at room temperature for 24 hours for complete drying. FT-Raman spectra were obtained for SLN (solid lipid nanoparticles without CEPc), SLN-CEPc, C-SLN (chitosan-coated solid lipid nanoparticles without CEPc), C-SLN-CEPc, and CEPc by using FT-Raman Spectrometer (FT -Ram II Bruker® Vertex 70v) in the range from 400 to 4000 cm^{-1} with a resolution of 4 cm^{-1}. In addition, thermograms for the nanoparticles (SLN, SLN-CEPc, C-SLN, C-SLN-CEPc) and CEPc were achieved using differential scanning calorimetry (DSC, Perkin Elmer 4000). For that, samples of approximately 10 mg were heated from 30 to 300°C in a closed aluminum sample holder at 10°C/min under a nitrogen gas flow of 50 mL/min.

In vitro release test

The release test was carried out for SLN-CEPc and C-SLN-CEPc samples in phosphate buffer saline (PBS) solutions at pH 7.4 and 1.2 containing Tween 80 at 1.0% w/v. The samples were added to the buffer solution and evaluated for 72 h at pH 7.4 and for 2 h at pH 1.2 at different time intervals. The samples were kept in constant agitation at 500 rpm at 37°C and the suspension was subjected to centrifugation (Eppendorf 5810 R) after predetermined intervals in a 30 kDa regenerated-cellulose ultrafilter (Amicon 0.5 mL - Millipore®) at 3,500 rpm for 15 minutes to separate the piperlonguminine released from SLN-CEPc and C-SLN-CEPc. The amount of free piperlonguminine was then quantified by HPLC-PDA.

Cytotoxicity in Vero cells and Hemolytic Activity

To analyze the cytotoxicity, confluent Vero cells (ATCC CCL81) were exposed to different concentrations (15.1-500 µg/mL) of SLN, SLN-CEPc, C-SLN, C-SLN-CEPc, and CEPc for 72 h, at 37°C and 5% of CO_2. After incubation, cell viability was assessed by the assay MTT (3-(4,5-dimethylthiazol-2yl)-2,5-diphenyl tetrazolium bromide). The 50% cytotoxic concentration (CC_{50}), a concentration at which the cell viability is reduced to 50%, was calculated in relation to the untreated controls (Benassi-Zanqueta *et al*., 2018).

Anti-Mycobacterium tuberculosis activity

An *in vitro* test to determine the minimum inhibitory concentration (MIC) in *M. tuberculosis* $H_{37}Rv$

(ATCC 27294) was also performed for SLN, SLN-CEPc, C-SLN, C- SLN-CEPc, and CEPc by using the Resazurin Microtiter Assay Plate (REMA) methodology (Palomino *et al*., 2002; Scodro *et al*., 2015). The samples were diluted in Middlebrook 7H9 supplemented with oleic acid, albumin, dextrose and catalase (OADC) enrichment (BBL/Becton-Dickinson, Sparks, MD, USA) in order to achieve final concentrations ranging from 0.39 to 100 µg/mL. Isoniazid was used as the reference drug in concentrations within the range from 0.007 to 1.0 µg/mL, whereas resazurin was used as an indicator of bacillary viability. MIC was thus defined as the lowest concentration of the drug which was capable of preventing the color change from blue to pink, (i.e. the absence of bacillary viability).

Statistical Analysis

The results were all presented as average ± standard deviation. The data were processed and submitted to analysis of variance (ANOVA), and the differences between the averages were determined by the Tukey test at the significance level of 5%.

RESULTS AND DISCUSSION

Characterization of SLN-CEPc e C-SLN-CEPc

The results for average diameter, PI, Zeta potential, EE, and loading capacity (LC) are shown in Table No. 1. In Figure No. 1A and Figure No. 1B, the images obtained by TEM for SLN-CEPc and C-SLN-CEPc formulations can be observed. It is worth mentioning that this is the first study of the encapsulation of the crude extract of *P. corcovadensis* in solid lipid nanoparticles for oral administration for the treatment of tuberculosis.

Table No. 1
Characterization of the solid lipid nanoparticles loaded with the crude extract of *Piper corcovadensis* roots

	SLN	SLN-CEPc	C-SLN	C- SLN-CEPc
Average diameter (nm)	69	82	164	164
Polydispersity index (-)	0.31	0.26	0.29	0.25
Zeta potential (mV)	-22.57	-22.80	40.20	29.60
pH (-)	6.87	6.25	6.01	5.74
Encapsulation efficiency (%)	-	94.50	-	97.02
Loading capacity (mg of CEPc/mL of nanoparticles suspension)	-	4.2	-	4.3

SLN: solid lipid nanoparticles without CEPc: SLN-CEPc: solid lipid nanoparticles loaded with crude extract of *Piper corcovadensis* roots; C-SLN: chitosan-coated solid lipid nanoparticles without CEPc; C-SLN-CEPc: chitosan-coated solid lipid nanoparticles loaded with crude extract of *P. corcovadensis* roots

By the qualitative analysis of nanoparticles' suspensions, one may notice that the systems showed a clear and homogeneous appearance, without any sign of phase separation. The SLN-CEPc presented an average diameter of 82 nm with a PI of 0.26, which shows that the CEPc incorporated in the SLN promoted an increase in the average diameter when compared with SLN (69 nm and PI: 0.31). The coating of the nanoparticles with chitosan also resulted in an increase in the average diameter of C-SLN-CEPc (164 nm and PI: 0.25) in comparison to SLN and SLN-CEPc, which is probably related to a rearrangement of the lipid matrix caused by the presence of chitosan (Vieira *et al*., 2018). The SLN-CEPc and C-SLN-CEPc showed PI less than 0.3, indicating adequate homogeneity in the particle size distribution so that they can be considered as monodisperse systems (Nemen & Lemos-Senna, 2011; Shazly, 2017). By TEM images (Figure No. 1), it could be observed that, for both formulations, the particles were spherical and not agglomerated. Furthermore, it was possible to confirm that the average diameter was below 200 nm, as previously determined by the dynamic light scattering analysis. It is worth mentioning that the size of the particles plays an important role in gastrointestinal absorption and excretion by the reticuloendothelial system. Considering oral administration, a particle size below 300 nm would be recommended for intestinal absorption (Das & Chaudhury, 2011). The average diameter achieved for SLN-CEPc and C-SLN-CEPc is thus in agreement with the values reported in the literature, where the SLN typically present a spherical morphology (Attama *et al*., 2012; Naseri *et al*., 2015).

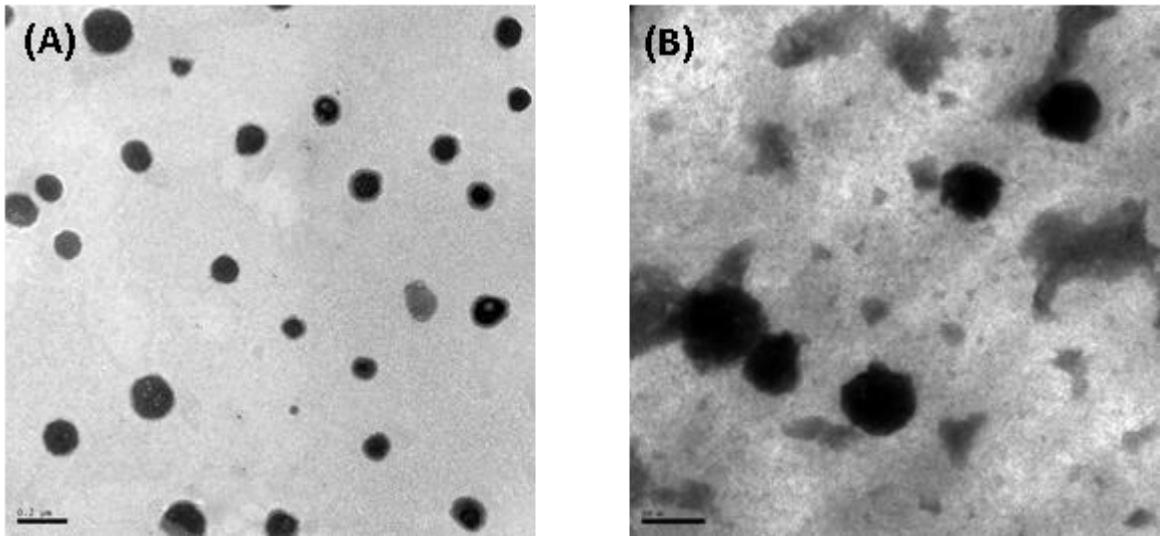

Figure No. 1
Images from transmission electron microscopy of (A) SLN-CEPc, (B) C-SLN-CEPc. (Scale bar: 0.2 µm)

The SLN-CEPc and C-SLN-CEPc showed Zeta potentials of -22.80 and 29.60 mV, respectively. The negative charge of the SLN-CEPc system can be explained by the fact that there is phospholipid in its composition (Schaffazick *et al*., 2003). Moreover, it could be noticed that the CEPc encapsulation did not affect the surface charge of the SLN-CEPc comparing with the SLN. On the other hand, the C-SLN-CEPc system showed a positive charge, representing a variation in relation to the SLN-CEPc, due to the presence of chitosan, which presents a positive charge in its molecule. The encapsulation of CEPc in C-SLN-CEPc led to a decrease in the Zeta potential compared with C-SLN. Vieira *et al*. (2018) have reported that the incorporation of the may occur by adsorption on the surface of solid lipid nanoparticles and thus causing a decrease in the Zeta potential. The positive charge of the solid lipid nanoparticles favors the interaction with the negative charge of intestinal epithelial membranes and mucosa, which in turn promotes a greater interaction, adhesion, and retention of the pharmaceutical form (Lima *et al*., 2018).

Since the Zeta potential reflects the charge on the surface of the particles, it is an important parameter to determine the stability of colloidal suspensions. For good stability, the Zeta potential value required is > ± 30 mV, so that adjacent particles are repelled and thus are less likely to form aggregates due to occasional collisions. Besides, these characteristics of the surface charge of particles may also influence the biological response of the drug. So, it can be said that the value found in the present study is very close to the required one, indicating that the SLN-CEPc and C-SLN-CEPc systems are less likely to aggregate (Schaffazick *et al*., 2003; Patel & Prajapati, 2016; Shah *et al*., 2017).

The chemical characterization of SLN-CEPc and C-SLN-CEPc by HPLC-PDA showed encapsulation efficiencies of 94.50 and 97.02%, respectively. In addition, the concentration of CEPc in SLN-CEPc and C-SLN-CEPc was 4.2 mg CEPc/mL of nanoparticles suspension (Table No. 1). The encapsulation efficiency was satisfactory, since the solid lipid nanoparticles' system is an ideal nanocarrier for lipophilic substances, due to the interaction of its nonpolar nucleus through hydrophobic forces, thus increasing the encapsulation efficiency (Xue *et al*., 2017).

To identify and verify CEPc-excipient interactions in the solid-state nanoparticles, FT-Raman analysis was performed, as shown in Figure No. 2, wherein the FT-Raman spectra of SLN, SLN-CEPc, C-SLN, C-SLN-CEPc, and CEPc can be observed. The samples were also evaluated by differential scanning calorimetry, as presented in the thermograms of Figure No. 3.

The SLN-CEPc and C-SLN-CEPc spectra showed bands at 1141 and 1146, 1298 cm^{-1}, which are related to the presence of a C-O bond at 1442 cm^{-1} which in turn is related to a stretch of the aromatic ring C=C. Bands at 1604 and 1608, 1654

and 1655 cm^{-1} related to the presence of the bonds N-H (bending) and C=O (stretching), and bands at 2882-2884 cm^{-1} related to a stretching of bonds of C-H (sp^3), C-H (sp^2) and N-H were also observed. These signs were characteristic of the presence of amides present in the CEPc.

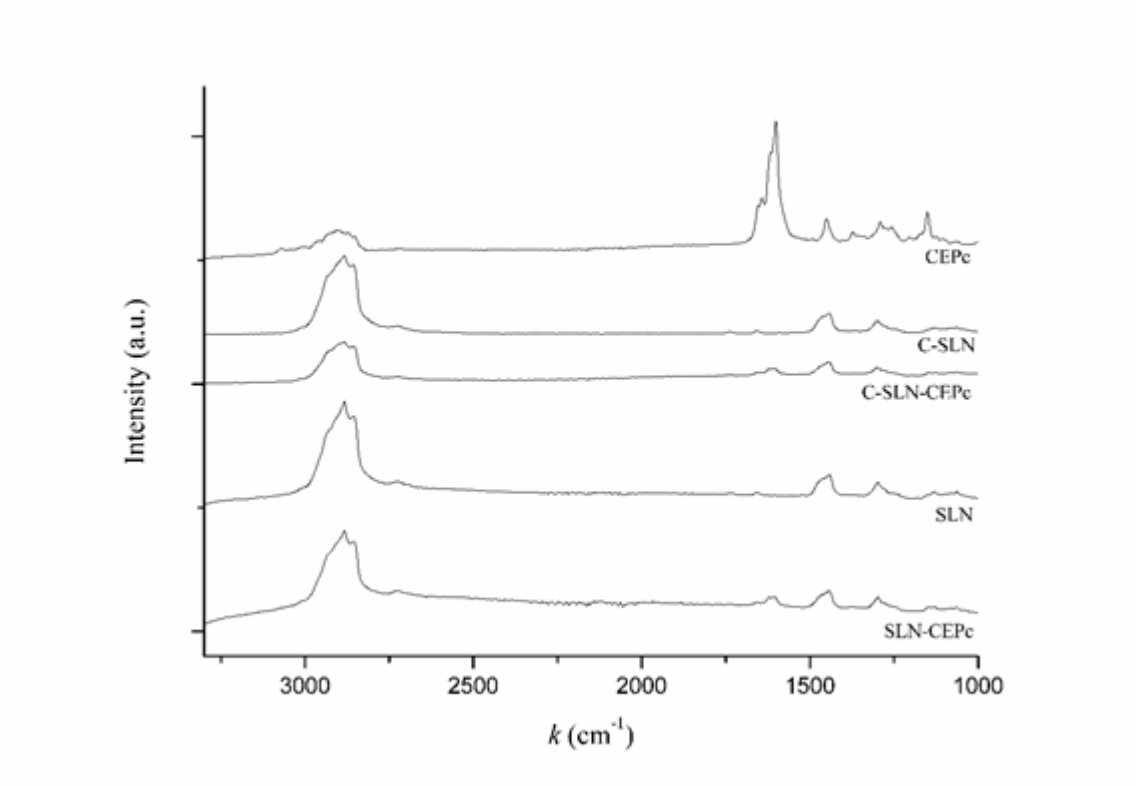

Figure No. 2
FT-Raman Spectra of solid lipid nanoparticles loaded with crude extract of *Piper corcovadensis* roots (SLN-CEPc), solid lipid nanoparticles without CEPc (SLN), chitosan-coated solid lipid nanoparticles loaded with crude extract of *Piper corcovadensis* roots (C-SLN-CEPc), chitosan-coated solid lipid nanoparticles without CEPc (C-SLN) and crude extract of *Piper corcovadensis* roots (CEPc).

Regarding the excipients, SLN-CEPc and C-SLN-CEPc spectra exhibited characteristic signs of the constituents that were present, with bands at 2884 and 2882, 2852 and 2851, 2724 and 2725 cm^{-1} related to stretching and bending of C-H bonds (sp^3), bands at 1740 and 1735 cm^{-1} related to a stretching of the ester group, bands at 1442 and 1443 that can be assigned to the stretching of CH_2-CH_2 bonds and bands at 1127 and 1130 and 1062 and 1064 cm^{-1} ascribed to a C-O stretching. Moreover, bands at 1082 and 1080 cm^{-1} related to the stretching of the bonds P=O and P-O-C were also observed (Yu *et al*., 2014; Agarwal *et al*., 2014; Pezeshki *et al*., 2014; Reham *et al*., 2015; Catauro *et al*., 2016). The spectra from SLN-CEPc and C- SLN-CEPc presented characteristic bands of the interaction between CEPc and the excipients. For this reason, these spectra were considered as the sum of CEPc and excipient bands. Regarding the physical mixture, the spectrum was the sum of the characteristic bands of the excipients. Besides that, by analyzing the FT-Raman spectra, no signs of a new chemical bond between the asset and the excipients could be observed, due to the absence of new bands.

In the DSC thermograms, the crude extract presented a wide endothermic peak around 50°C, which is possibly assigned to a loss of volatile material of the sample, with a characteristic pattern of thermal degradation from 142°C. The main melting peak of Precirol® ATO 5 was achieved at 53°C, which is in line with the results found in the literature (Devi & Argawal, 2019). The incorporation of the extract did not lead to expressive alterations on the thermal behavior of the nanoparticles, which is probably due to the low concentration used. Lecithin (phospholipon® 90G) is liquid at room temperature and therefore could not be detected in that analysis. Furthermore, the presence of chitosan did not change

the melting temperature of the encapsulating lipid, corroborating the hypothesis that it is deposited on the surface of the nanoparticles.

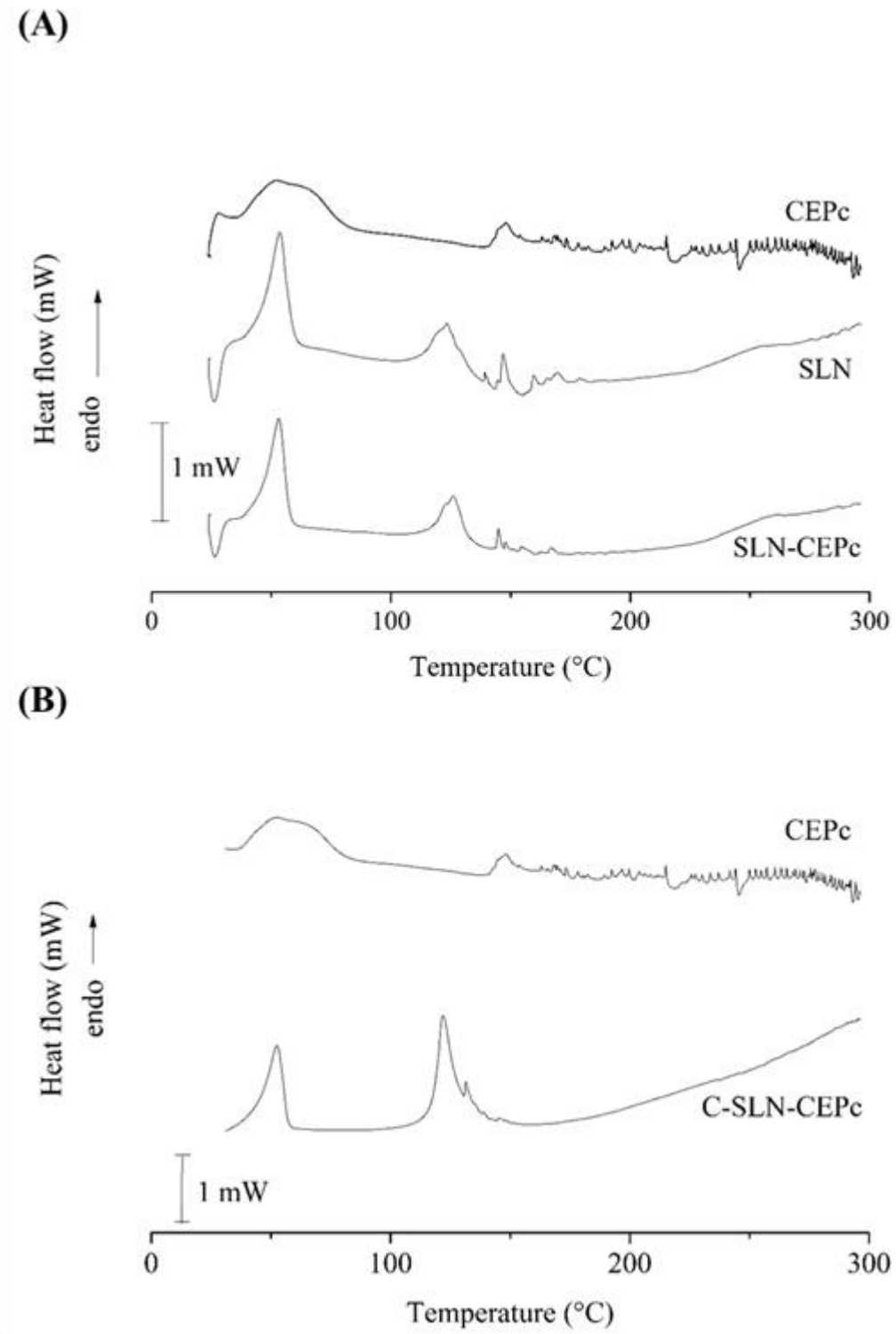

Figure No. 3

Thermograms of the nanoparticles and crude extract of *Piper corcovadensis* roots obtained by Differential Scanning Calorimetry. (A) Solid lipid nanoparticles loaded with crude extract of *Piper corcovadensis* roots (SLN-CEPc), solid lipid nanoparticles without CEPc (SLN), and crude extract of *Piper corcovadensis* roots (CEPc). (B) Chitosan-coated solid lipid nanoparticles loaded with crude extract of *Piper corcovadensis* roots (C-SLN-CEPc) and crude extract of *Piper corcovadensis* roots (CEPc).

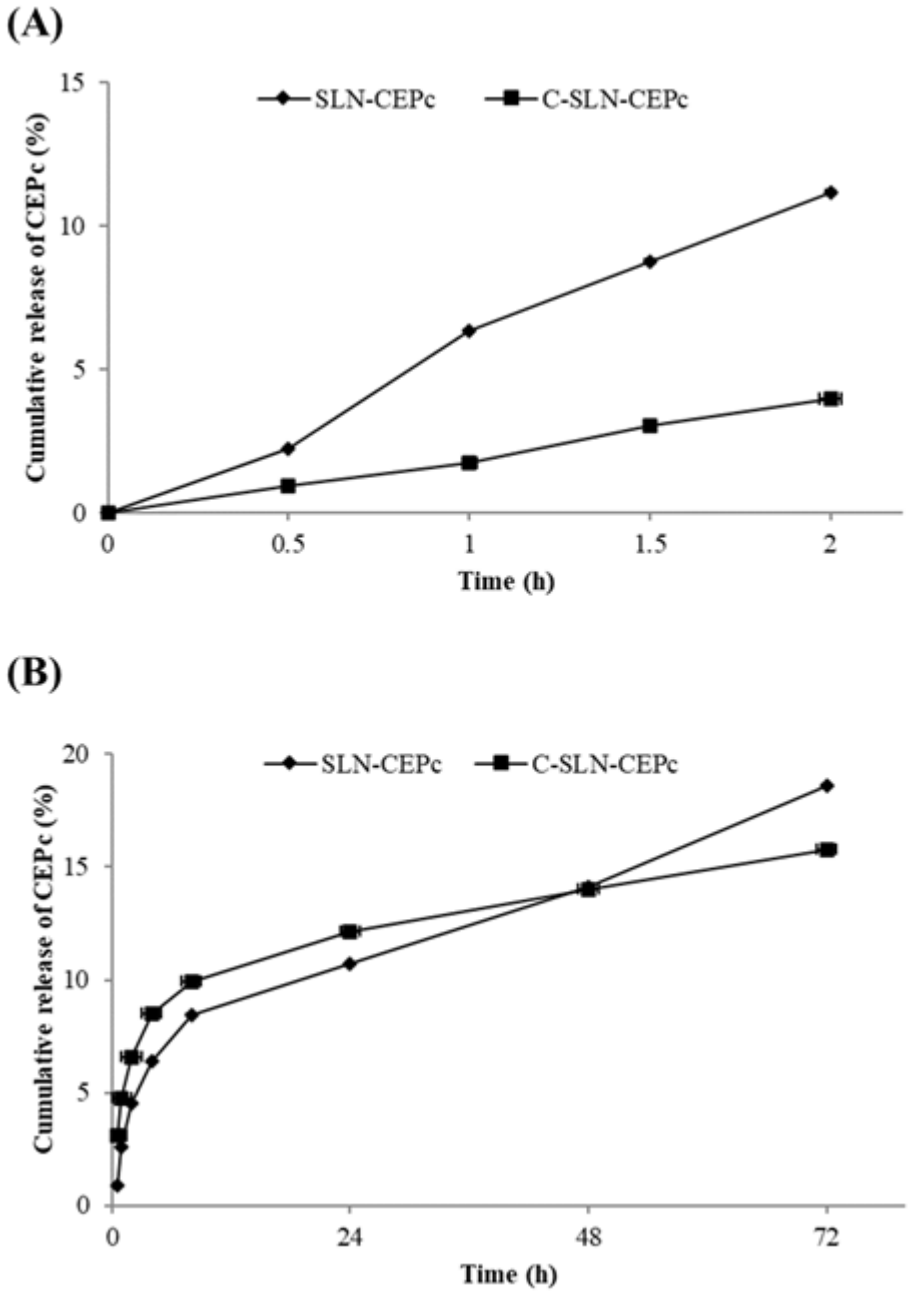

Figure No. 4
Release profile of SLN-CEPc and C- SLN-CEPc at pH 1.2 for 2 h (A) and at pH 7.4 for 72 h (B)

In summary, by observing the results achieved for average diameter, Zeta potential, the images and the DSC thermograms of the nanoparticles, it can be suggested that the coating of the SLN-CEPc with chitosan by surface modification took place. These results demonstrate that the emulsification method by melting, the chosen proportion of solid lipids and surfactants and the chitosan-coating were suitable for the development of SLN-CEPc and C-SLN-CEPc as systems for modified drug release.

In vitro release test

The SLN-CEPc and C-SLN-CEPc *in vitro* release tests were performed by using phosphate-saline buffer (PBS) simulating the gastrointestinal pH: pH 1.2 (stomach) and pH 7.4 (intestine), to represent the passage of the nanoparticles after oral administration.

The results are shown in Figure No. 4.

Both SLN-CEPc and C-SLN-CEPc showed a low CEPc-release profiles. At pH 1.2, the SLN-CEPc and C-SLN-CEPc presented different release profiles up to 2 h (Figure No. 4A). C-SLN-CEPc showed a slower CEPc release profile (4% in 2 h) compared with the SLN-CEPc (11% in 2 h). At pH 7.4, both formulations released less than 10% of encapsulated CEPc in the first 8 h, gradually increasing up to 72 h. However, after 72h, the release of CEPc was less than 20% (Figure No. 4B). According to literature reports, the release profile of pharmaceuticals from nanoparticles may be affected by several factors, such as the solubility and the partition coefficient of the drug, the nature of the lipids used, parameters of production and surface modification (Baek & Cho, 2017). The surface modification of the SLN-CEPc with chitosan may be a promising technique to inhibit the release of CEPc in acidic conditions providing thus protection against degradation and improving the bioavailability of the drug (Baek & Cho, 2017). These results indicate that most part (> 80%) of the CEPc remained in SLN-CEPc and C-SLN-CEPc after the contact with the gastrointestinal mimetic conditions, which may contribute to the release of CEPc within the target cells.

Stability tests

The stabilities of SLN-CEPc and C-SLN-CEPc were verified at temperatures of 5, 30, and 40ºC for 15, 30, 60, and 90 days and the physicochemical parameters of average diameter, PI, and Zeta potential were analyzed, as can be seen in Tables No. 2 and Table No. 3. The data obtained 24 hours after preparing the formulations were the base values used for the comparisons.

Table No. 2
Average diameter, polydispersity index, and Zeta potential of the solid lipid nanoparticles loaded with crude extract of *Piper corcovadensis* roots (SLN-CEPc) for stability studies

Temperature	5ºC					30ºC				40ºC			
Days	1	15	30	60	90	15	30	60	90	15	30	60	90
Parameter													
Average diameter (nm)	80^{c}	99^{c}	136^{b}	137^{b}	140^{b}	96^{c}	188^{a}	-	-	90	-	-	-
Polydispersity index	0.32^{a}	0.30^{a}	0.31^{a}	0.32^{a}	0.32^{a}	0.30^{a}	0.24^{a}	-	-	0.28^{a}	-	-	-
Zeta potential (mV)	-24.30^{a}	-24.7^{a}	-24.5^{a}	-26.1^{a}	-24.4^{a}	-24.8^{a}	-20.3^{b}	-	-	-27.0^{a}	-	-	-

-: not determined. The average values followed by the same letter on a line do not differ from each other according to the Tukey test ($p \leq 0.05$)

Long-term stability studies are performed to establish or confirm the expiration date and recommend the storage conditions resulting from the checking of the physical, chemical, biological and microbiological characteristics of a pharmaceutical product during or after the expected expiration date (Brasil, 2005).

The SLN-CEPc system (Table No. 2) stored at different temperatures varied, presenting turbidity and phase separation at 30ºC (30 days) and 40ºC (15 days), which indicates the destabilization of the system. In the SLN-CEPc formulation stored at 30ºC, there was an increase in the average particle diameter (188 nm) in the Zeta potential (-20.3 mV). At high temperatures, the kinetic energy of the system increases, leading to an increase of the number of collisions between particles, favoring thus aggregation and, consequently, an increase in the particle diameter (Freitas & Müller, 1999). A destabilization process associated with changes in the Zeta potential can cause an increase in the average particle diameter by aggregation, namely by the attraction between adjacent particles due to occasional collisions (Shah *et al*., 2017). The increase in temperature may cause a decrease in the micro-viscosity of the emulsifier and lead to a destabilization of the system since a high rigidity of the emulsifier's film (micro-viscosity) prevents the fusion of the film layers after the contact between particles (Schuhmann, 1995).

When stored at 5ºC, the SLN-CEPc formulation was more stable. On the other hand, an increase in the average particle diameter from 80 to 140 nm could be observed. Low temperatures might favor the aggregation of particles, this occurs mainly due to the decrease in the Brownian motion of the particles, which in turn leads to increased interaction (collisions) and interparticle reaction (Santos *et al*., 2015). The stability of C-SLN-CEPc (Table No. 3) significantly varied (p<0.05) at different temperatures (5; 30 and 40ºC) within the analyzed parameters. Nevertheless, in the macroscopic analysis, a system with a clear and homogeneous aspect without separation of phases or turbidity could be noticed, showing that it remained stable at the end of 90 days. These changes may be related to the chitosan-coating, which after the time in aqueous suspension may have dissolved, causing thus changes in the stability parameters.

Table No. 3
Average diameter, polydispersity index, and Zeta potential of the chitosan-coated solid lipid nanoparticles with crude extract of *Piper corcovadensis* roots (C-SLN-CEPc) for stability studies

Temperature	5ºC					30ºC				40ºC			
Days	1	15	30	60	90	15	30	60	90	15	30	60	90
Parameter													
Average diameter (nm)	164^{a}	154^{b}	132^{d}	133^{d}	121^{e}	141^{c}	115^{e}	107^{f}	91^{g}	100$^{f\backslash}$	93$^{f.g}$	103^{f}	99^{f}
Polydispersity index	0.25^{a}	0.26^{a}	0.29^{a}	0.28^{a}	0.31^{a}	0.28^{a}	0.29^{a}	0.24^{a}	0.29^{a}	0.29^{a}	0.28^{a}	0.25^{a}	0.23^{a}
Zeta potential (mV)	29.6^{a}	27.7^{a}	27.1^{a}	17.0$^{a.b}$	8.0^{c}	25.4^{a}	21.5^{a}	12.4^{b}	5.4^{c}	23.7^{a}	21.0^{a}	11.7^{b}	8.6^{c}

-: not determined. The average values followed by the same letter on a line do not differ from each other according to the Tukey test (p≤0.05)

Regarding the developed systems, C-SLN-CEPc proved to be more stable at high temperatures, due to the presence of chitosan, which is an amphiphilic polyelectrolyte and combines electrosteric and viscosifying stabilization mechanisms that may increase the stability of nanoparticle dispersions (Ridolfi *et al*., 2012). The aqueous stability of the SLN-CEPc and C-SLN-CEPc suspensions was determined by evaluating average diameter, polydispersity index, and Zeta potential, depending on the pH change of the aqueous medium.

The stability of the nanoparticle dispersions was also evaluated at different pH ranges. The data of average diameter and Zeta potential of the SLN-CEPc and C-SLN-CEPc nanoparticles at different pH values are shown in Figure No. 5.

In the SLN-CEPc suspension, with an increase in pH, there was an increase in the average diameter of the nanoparticles (85 and 94 nm, respectively) when compared the average diameter of the particles at pH 3.0; 5.0, and 6.0. At acidic pH (pH 3.0), there was an enhancement of the Zeta potential (-3.4 mV). The suspension of C-SLN-CEPc with decreasing pH (pH 3.0) showed a decrease in the average diameter of the nanoparticles (83 nm). In the other pH ranges, there were no significant changes (p<0.05) in the parameters evaluated.

Stability and dispersibility of the aqueous nanoparticles' suspension are important for the long-term stability of the lipid particle and the retention of the core material (Choi *et al*., 2014). Alterations in pH can easily destabilize or flocculate the SLN since they have an electrical double layer on their surface, where the first layer contains ions adsorbed directly on the particle, and in the second one, the ions are attached to the surface charge. So, the more away from the isoelectric point the pH is, independent of positive or negative state, the charge density of a particle it increases, as has been reported for ionic and amphoteric surfactants elsewhere (Schwenzfeier *et al*., 2013). Choi *et al*. (2014) reported that the particle diameter increased with a decrease in the pH of the nanoparticle suspension. The authors suggest that this increase may be due to the protonation of the ether bond in polyoxyethylene chains of the emulsifier (Tween 80), which at an acidic condition

causes insufficient interfacial adsorption of the surfactant between lipid and aqueous phases, and this may lead to a decrease in the surfactant's surface properties, changing thus the electrical charge of the bilayer leading to the aggregation of particles.

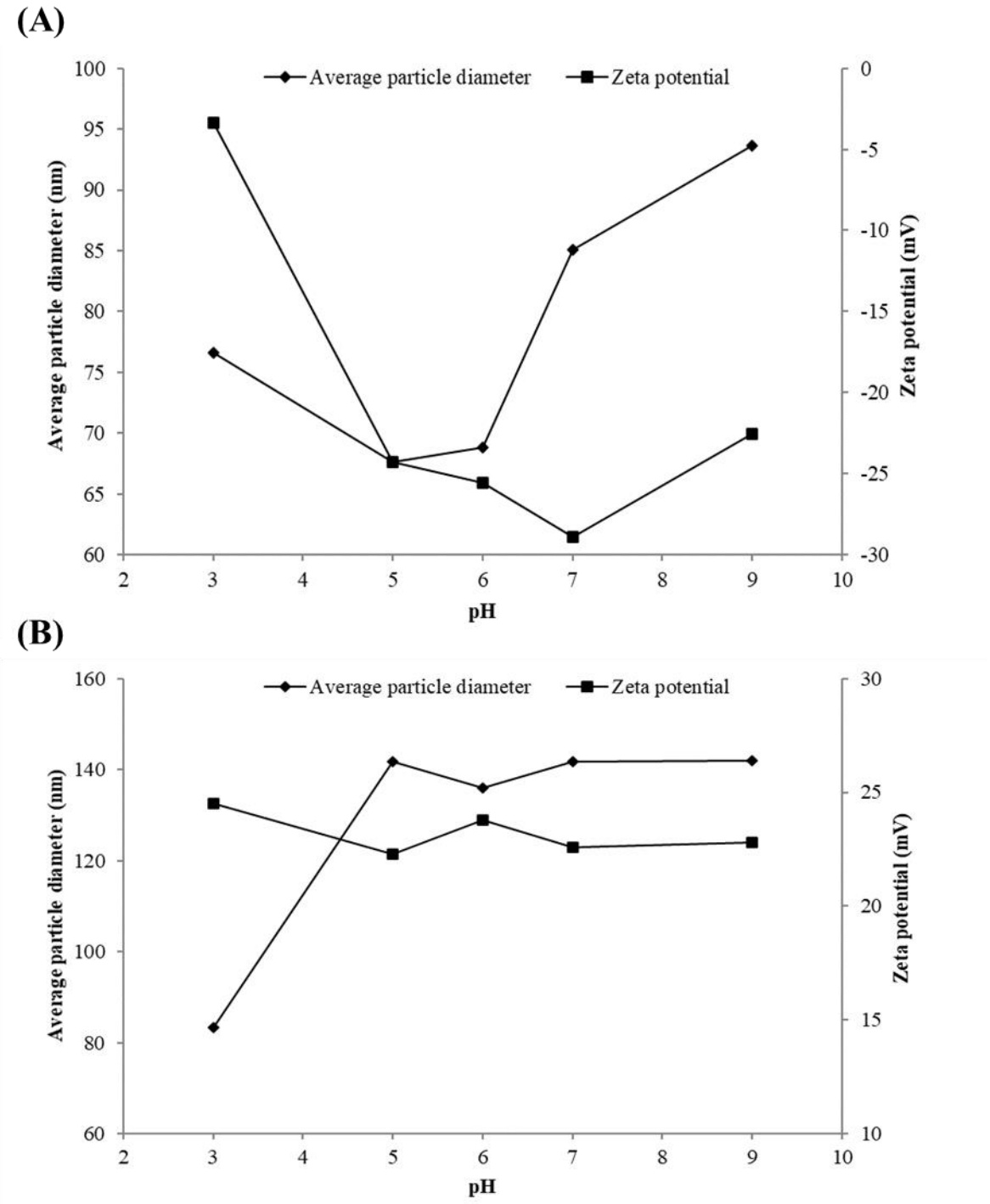

Figure No. 5
Stability of the nanoparticles at different pH values in relation to average diameter and Zeta potential

Biological activity

The minimum inhibitory concentration (MIC) for *M. tuberculosis* and the 50% cytotoxic concentration (CC_{50}) in Vero cells of SLN, SLN-CEPc, C-SLN, C-SLN-CEPc, and CEPc are presented in Table No. 4.

The SLN-CEPc and C-SLN-CEPc showed MIC values of 12.5 µg/mL and CC_{50} of 60.0 and 70.0 µg/mL, respectively, whereas CEPc showed a MIC of 15.6 µg/mL and CC_{50} of 55 µg/mL. Both SLN-CEPc and C-SLN-CEPc showed promising results and the encapsulation of CEPc did not inhibit their antimycobacterial activities, since they showed similar anti-*M. tuberculosis* action. The SLN system showed no action against *M. tuberculosis* in the highest concentration tested, while the C-SLN exhibited antimycobacterial action (MIC: 100 µg/mL), which may be due to the presence of chitosan, that presents antimicrobial activity (Ridolfi *et al*., 2012).

Table No. 4
Minimum inhibitory concentration (MIC) in *Mycobacterium tuberculosis* ($H_{37}Rv$) and cytotoxicity in Vero cells of the solid lipid nanoparticles loaded with crude extract of *Piper corcovadensis*

Samples	MIC (µg/mL)	CC_{50} (µg/mL)
SLN	>100	70.3
SLN-CEPc	12.5	60.0
C-SLN	100.0	78.7
C- SLN-CEPc	12.5	70.0
CEPc	15.6	71.9

MIC: Minimum inhibitory concentration; CC_{50}: 50% cytotoxic concentration; SLN: solid lipid nanoparticles without CEPc: SLN-CEPc: solid lipid nanoparticles loaded with crude extract of *Piper corcovadensis* roots; C-SLN: chitosan-coated solid lipid nanoparticles without CEPc; C-SLN-CEPc: chitosan-coated solid lipid nanoparticles loaded with crude extract of *P. corcovadensis* roots; CEPc: crude extract of *Piper corcovadensis* roots

The hemolysis assay in erythrocytes of sheep was carried out, from which it could be observed that SLN-CEPc and C-SLN-CEPc did not show hemolytic effect at the evaluated concentrations after 60 minutes of incubation. Hemolysis of 13.8% and 0.4% were achieved at 100 µg/mL for SLN and C-SLN, respectively. However, at the concentrations of 50, 25, and 12.5 µg/mL they did not exhibit any hemolytic effect. Thus, at the concentration of 12.5 µg/mL (MIC for *M. tuberculosis*) none of the formulations showed hemolytic effects.

SLN-CEPc and C-SLN-CEPc showed antimycobacterial activity against *M. tuberculosis.* The cell wall of *M. tuberculosis* presents on its surface a coating composed mainly of mycolic acids, which are in turn composed of long chains of fatty acids, that confer a low permeability to hydrophobic substances (Lemmer *et al*., 2015). Since the nanoparticles are composed of lipids and phospholipids, they allow a greater lipophilicity to the system, interacting with the mycobacterial cell wall and penetrating it due to its small size and hydrophobic character, releasing thus the drug more efficiently (Aboutaleb *et al*., 2012).

CONCLUSION

Solid lipid nanoparticles were obtained as an alternative to the oral administration of the crude extract of *Piper corcovadensis* roots. The nanoparticles showed high encapsulation efficiency, constituting monodispersed systems with stable, nanometric, and spherical particles, without particle aggregation. The surface modification of nanoparticles by chitosan-coating was successful, improving its stability and cytotoxicity. It was noticed that temperature and pH influence the stability of the aqueous dispersions of the nanoparticles.

The antimycobacterial activity of the system against *M. tuberculosis* was assessed *in vitro* and showed promising results. Neither the nanoparticles nor the extract exhibited hemolytic and cytotoxic effects in Vero cells. These results demonstrate that nanoencapsulation proved to be satisfactory and that its use in the development of new products is justifiable.

ACKNOWLEDGEMENTS

This work was supported through grants from the CNPq (*Conselho Nacional de Desenvolvimento*

Científico e Tecnológico), CAPES (*Capacitação de Aperfeiçoamento de Pessoal de Nível Superior*), COMCAP (*Complexo de Centrais de Apoio a Pesquisa*) of Universidade Estadual de Maringá (UEM) and *Central Analítica Multiusuário* of Universidade Tecnológica Federal do Paraná (CAMulti-CM) for the Scanning Calorimetry Analysis.

REFERENCES

Aboutaleb E, Noori M, Gandomi N, Atyabi F, Fazeli MR, Jamalifar H, Dinarvand R 2012. Improved antimycobacterial activity of rifampin using solid lipid nanoparticles. **Int Nano Lett** 2: 33. **https://doi.org/10.1186/2228-5326-2-33**

Agarwal A, Kharb V, Saharan VA. 2014. Process optimisation, characterisation and evaluation of resveratrol-phospholipid complexes using Box-Behnken statistical design. **Int Curr Pharm** 3: 301 - 308. **https://doi.org/10.3329/icpj.v3i7.19079**

Attama AA, Momoh MA, Builders PF. 2012. **Lipid nanoparticulate drug delivery systems: a revolution in dosage form design and development**. In: Sezer AD. Ed. Pharmacology, toxicology and pharmaceutical science. InTech Open Access Publisher, Croatia.

Baek JS, Cho CW. 2017. Surface modification of solid lipid nanoparticles for oral delivery of curcumin: Improvement of bioavailability through enhanced cellular uptake, and lymphatic uptake. **Eur J Pharm Biopharm** 117: 132 - 140. **https://doi.org/10.1016/j.ejpb.2017.04.013**

Benassi-Zanqueta E, Marques CF, Nocchi SR, Dias Filho BP, Nakamura CV, Ueda-Nakamura T. 2018. Parthenolide Influences *Herpes simplex virus* 1 Replication *in vitro*. **Intervirology** 61: 14 - 22. **https://doi.org/10.1159/000490055**

Brasil. 2005. Ministério da Saúde, ANVISA - Agência Nacional de Vigilância Sanitária, 2005. RE Nº 1, de 29/07/2005, **Guia para a Realização de Estudos de Estabilidade**, MS: Brasília.

Brasil. 2017. Ministério da Saúde, ANVISA - Agência Nacional de Vigilância Sanitária, 2017. RE Nº 166, de 24/07/2017, **Guia para validação de métodos analíticos e bioanalíticos**, MS: Brasília.

Catauro M, Bollino F, Nocera P, Piccolella S, Pacifico S. 2016. Entrapping quercetin in silica/polyethylene glycol hybrid materials: Chemical characterization and biocompatibility. **Mater Sci Eng C** 68: 205 - 212. **https://doi.org/10.1016/j.msec.2016.05.082**

Choi KO, Aditya NP, Ko S. 2014. Effect of aqueous pH and electrolyte concentration on structure, stability and flow behavior of non-ionic surfactant based solid lipid nanoparticles. **Food Chem** 147: 239 - 244. **https://doi.org/10.1016/j.foodchem.2013.09.095**

Das S, Chaudhury A. 2011. Recent advances in lipid nanoparticle formulations with solid matrix for oral drug delivery. **AAPS PharmSciTech** 12: 62 - 76. **https://doi.org/10.1208/s12249-010-9563-0**

Deore RK, Kavitha K, Tamizhmani TG. 2010. Preparation and evaluation of sustained release matrix tablets of tramadol hydrochloride using glyceryl palmitostearate. **Trop J Pharm Res** 9: 275 - 281. **https://doi.org/10.4314/tjpr.v9i3.56289**

Devi R, Agarwal S. 2019. Some multifunctional lipid excipients and their pharmaceutical applications. **Int J Pharm Pharm Sci** 11: 2019. **https://doi.org/10.22159/ijpps.2019v11i9.34194**

Facundo VA, Morais SM, Braz Filho R. 2004. Chemical constituents of *Ottonia corcovadensis* Miq. from Amazon forest: ^{1}H and ^{13}C chemical shift assignments. **Quím Nova** 27: 79 - 83. **https://doi.org/10.1590/S0100-40422004000100017**

Fernandez CMM, Baldin VP, Ieque AL, Bernuci KZ, Almeida RT, Valone LM, Fonseca DP, Makimori RY, Andrade JPP, Pilau EJ, Romagnolo MB, Nakamura TU, Cardoso RF, Cortez DAG, Gazim ZC, Scodro RBL, Dias Filho BP. 2019. Anti-*Mycobacterium tuberculosis* activity of dichloromethane extract of *Piper corcovadensis* (Miq.) C. DC. roots and isolated compounds. **Ind Crop Prod** 131: 341 - 347. **https://doi.org/10.1016/j.indcrop.2019.01.064**

Freitas C, Müller RH. 1999. Correlation between long-term stability of solid lipid nanoparticles (SLN) and crystallinity of the lipid phase. **Eur J Pharm Biopharm** 47: 125 - 132. **https://doi.org/10.1016/s0939-6411(98)00074-5**

Geszke-Moritz M, Moritz M. 2016. Solid lipid nanoparticles as attractive drug vehicles: composition, properties and therapeutic strategies. **Mater Sci Eng C** 68: 982 - 994. **https://doi.org/10.1016/j.msec.2016.05.119**

Jato JLV. 2009. **Nanotecnología farmacêutica, realidades y possibilidades farmacoterapéuticas**. Instituto de España, Real Academia Nacional de Farmacia, Monografía XXVIII, Madrid, España.

Lemmer Y, Kalombo L, Pietersen R-D, Jones AT, Semete-Makokotlela B, Van Wyngaardt S, Ramalapa B, Stoltz AC, Baker B, Verschoor JA, Swai HS, De Chastellier C. 2015. Mycolic acids, a promising mycobacterial ligand for targeting of nanoencapsulated drugs in tuberculosis. **J Control Rel** 211: 94 - 104. **https://doi.org/10.1016/j.jconrel.2015.06.005**

Lima IA, Khalil NM, Tominaga TT, Lechanteur A, Sarmento B, Mainardes RM. 2018. Mucoadhesive chitosan-coated PLGA nanoparticles for oral delivery of ferulic acid. **Artif Cell Nanomed B** 46: 993 - 1002. **https://doi.org/10.1080/21691401.2018.1477788**

Lin C.H, Chen C.H, Lin Z.C, Fang J.Y. 2017. Recent advances in oral delivery of drugs and bioactive natural products using solid lipid nanoparticles as the carriers. **J Food Drug Anal** 25: 219 - 234. **https://doi.org/10.1016/j.jfda.2017.02.001**

Marcato PD. 2009. Preparação, caracterização e aplicações em fármacos e cosméticos de nanopartículas lipídicas sólidas. **Rev Eletron Farm** 2: 1 - 37. **https://doi.org/10.5216/ref.v6i2.6545**

Mishra V, Bansal KK, Verma A, Yadav N, Thakur S, Sudhakar K, Rosenholm JM. 2018. Solid lipid nanoparticles: emerging colloidal nano drug delivery systems. **Pharmaceutics** 10: 191. **https://doi.org/10.3390/pharmaceutics10040191**

Naseri N, Valizadeh H, Zakeri-Milani P. 2015. Solid lipid nanoparticles and nanostructured lipid carriers: structure, preparation and application. **Adv Pharm Bull** 5: 305 - 313. **https://doi.org/10.15171/apb.2015.043**

Nemen D, Lemos-Senna E. 2011. Preparation and characterization of resveratrol-loaded lipid-based nanocarriers for cutaneous administration. **Quím Nova** 34: 408 - 413. **https://doi.org/10.1590/S0100-40422011000300008**

Palomino JC, Martin A, Camacho HG, Swings J, Portaels F. 2002. Resazurin microtiter assay plate: simple and inexpensive method for detection of drug resistance in *Mycobacterium tuberculosis*. **Antimicrob Agents Chemother** 46: 2720 - 2722. **https://doi.org/10.1128/aac.46.8.2720-2722.2002**

Parmar VS, Jain SC, Bisht KS, Rajni J, Poonam T, Amitabh J, Om DT, Ashok KP, Jesper W, Olsena CE, Bolla PM. 1997. Phytochemistry of the genus *Piper*. **Phytochemistry** 46: 597 - 673. **https://doi.org/10.1016/S0031-9422(97)00328-2**

Patel AN, Prajapati BG. 2016. Design and development of solid lipid nanoparticles (SLNs) of zolmitriptan for the treatment of migraine. **Eur J Biomed Pharm Sci** 3: 253 - 259.

Pereira AO, Avila JM, Carmo G, Siqueira FS, Campos MMA, Back DF, Morel AF, Dalcol II. 2018. Chemical composition, antimicrobial and antimycobacterial activities of *Aristolochia triangularis* Cham. from Brazil. **Ind Crop Prod** 121: 461 - 467.

Pezeshki A, Ghanbarzadeh B, Mohammadi M, Fathollahi I, Hamishehkar H. 2014. Encapsulation of vitamin A palmitate in nanostructured lipid carrier (nlc)-effect of surfactant concentration on the formulation properties. **Adv Pharm Bull** 4: 563 - 568. **https://doi.org/10.5681/apb.2014.083**

Reham SS, Masjuki HH, Kalam MA. 2015. FTIR and ^{1}H NMR analysis of water emulsified Palm biodiesel with Span 80. **Int J Eng Technol Manag Appl Sci** 3: 2015.

Ridolfi DM, Marcato PD, Justo GZ, Cordi L, Machado D, Durán N. 2012. Chitosan-solid lipid nanoparticles as carriers for topical delivery of tretinoin. **Colloids Surf B Biointerfaces** 93: 36 - 40. **https://doi.org/10.1016/j.colsurfb.2011.11.051**

Santos AD. 2015. **Caracterização e avaliação da citotoxidade de nanopartículas de ouro cobertas com citrato.** Thesis, Universidade de Brasília, Brasília, Brasil.

Schaffazick SR, Pohlmann AR, Dalla-Costa T, Guterres SS. 2003. Freeze-drying polymeric colloidal suspensions: nanocapsules, nanospheres and nanodispersion. A comparative study. **Eur J Pharm Biopharm** 56: 501 - 505. **https://doi.org/10.1016/S0939-6411(03)00139-5**

Schuhmann R. 1995. **Physikalische Stabilita¨t parenteraler Fettemulsionen—Entwicklung eines Untersuchungsschemas unter besonderem Aspekt analytischer Mo¨glichkeiten**. Thesis. Freie Universita¨t Berlin, Berlin, Germany.

Schwenzfeier A, Helbig A, Wierenga PA, Gruppen H. 2013. Emulsion properties of algae soluble protein isolate from *Tetraselmis* sp. **Food Hydrocoll** 30: 258 - 263. **https://doi.org/10.1016/j.foodhyd.2012.06.002**

Scodro RBL, Espelho SC, Pires CTA, Garcia VAS, Cardozo-Filho L, Cortez LER, Pilau EJ, Ferracioli KRC, Siqueira VLD, Cardoso RF, Cortez DAG. 2015. A new benzoic acid derivative from *Piper diospyrifolium* and its anti-*Mycobacterium tuberculosis* activity. **Phytochem Lett** 11: 18 - 23. **https://doi.org/10.1016/j.phytol.2014.10.015**

Shah MR, Imran M, Ullah S. 2017. **Lipid-based nanocarriers for drug delivery and diagnosis** (micro and nano technologies series). Kidlington, Inglaterra.

Shazly GA. 2017. Ciprofloxacin controlled-solid lipid nanoparticles: characterization, *in vitro* release, and antibacterial activity assessment. **Biomed Res Int** 2120734. **https://doi.org/10.1155/2017/2120734**

Trousil J, Filippov SK, Hrubý M, Mazel T, Syrová Z, Cmarko D, Svidenská S, Matějková J, Kováčik L, Porsch B, Konefał R, Lund R, Nyströmd B, Raškab I, Štěpánek P. 2017. System with embedded drug release and nanoparticle degradation sensor showing efficient rifampicin delivery into macrophages. **Nanomed Nanotechnol Biol Med** 13: 307 - 315. **https://doi.org/10.1016/j.nano.2016.08.031**

Vieira ACC, Chaves LL, Pinheiro S, Pinto S, Pinheiro M, Lima SC, Ferreira D, Sarmento B, Reais S. 2018. Mucoadhesive chitosan-coated solid lipid nanoparticles for better management of tuberculosis. **Int J Pharm** 536: 478 - 485. **https://doi.org/10.1016/j.ijpharm.2017.11.071**

WHO. World Health Organization, 2019. Global Tuberculosis Report 2019. Available in: **https://apps.who.int/iris/bitstream/handle/10665/329368/9789241565714-eng.pdf?ua=1**

Yu L, Xue W, Cui L, Xing W, Cao X, Li H. 2014. Use of hydroxypropyl-β-cyclodextrin/polyethylene glycol 400, modified Fe_3O_4 nanoparticles for congo red removal. **Int J Biol Macromol** 64: 233 - 239. **https://doi.org/10.1016/j.ijbiomac.2013.12.009**

Xue J, Wang T, Hu Q, Zhou M, Luo Y. 2017. A novel and organic solvente-free preparation of solid lipid nanoparticles using natural biopolymers as emulsifier and stabilizer. **Int J Pharm** 531: 59 - 66. **https://doi.org/10.1016/j.ijpharm.2017.08.066**